Re-Evaluating the Cannstatt Cranium (Germany): Using Geometric Morphometrics to Assess a Lost Presumed Human Fossil

BENJAMIN CHAMBERLAIN*
Palaeoanthropology, Institute for Archaeological Sciences, Eberhard Karls Universität Tübingen; and, Senckenberg Centre for Human Evolution and Palaeoenvironment, Eberhard Karls Universität Tübingen, Tübingen, GERMANY; ben.j.chamberlain@gmail.com

CAROLIN RÖDING
Palaeoanthropology, Institute for Archaeological Sciences, Eberhard Karls Universität Tübingen; and, Senckenberg Centre for Human Evolution and Palaeoenvironment, Eberhard Karls Universität Tübingen, Tübingen, GERMANY; carolin.roeding@uni-tuebingen.de

ALEX HUBBE
Staatliches Museum für Naturkunde Stuttgart, Rosenstein 1, 70191 Stuttgart, GERMANY; Departamento de Oceanografia, Instituto de Geociências, Universidade Federal da Bahia, R. Barão de Jeremoabo, S/N, 40170-020 Salvador, BA; and Instituto do Carste, Rua Barcelona 240/302, 30360-260 Belo Horizonte, MG, BRAZIL; alexhubbe@yahoo.com

KATERINA HARVATI*
Paleoanthropology, Institute for Archaeological Sciences, Eberhard Karls Universität Tübingen; Senckenberg Center for Human Evolution and Paleoenvironments, Eberhard Karls Universität Tübingen; DFG Center for Advanced Studies 'Words, Bones, Genes, Tools', Eberhard Karls Universität Tübingen; HUMAN ORIGINS – Cluster of Excellence for Integrative Human Origins Studies (EXC 3101), Eberhard Karls University of Tübingen, Tübingen, GERMANY; Centre for Early Sapiens Behaviour (SapienCE), University of Bergen, NORWAY; and, Museum of Anthropology, Medical School, National and Kapodistrian University of Athens, Athens, GREECE; katerina.harvati@ifu.uni-tuebingen.de

*corresponding authors: Benjamin Chamberlain; *ben.j.chamberlain@gmail.com; Katerina Harvati; katerina.harvati@ifu.uni-tuebingen.de*

submitted: 3 April 2025; revised 4 December 2025; accepted: 4 February 2026

Handling Editor in Chief: Karen Rosenberg

ABSTRACT

Originally suggested to represent a new group of hominins, the presumed fossil cranium from Cannstatt, Germany, was influential in early accounts of human evolution. Despite its early prominence, it was later reclassified as a modern human and subsequently fell into obscurity, after its destruction in World War II. Here we revisit the Cannstatt specimen using 3D geometric morphometrics to evaluate its morphology and taxonomic status using a cast of the original. A surface scan of the cast, along with a comparative dataset of 46 cranial specimens from Middle and Late Pleistocene hominins, as well as recent *Homo sapiens*, were used in the analysis. The results consistently indicated that Cannstatt aligns most closely with early *Homo sapiens*, also with significant similarities to recent *H. sapiens*. This supports its later assignment to *H. sapiens* and counters its initial classification as its own distinct race or a Neanderthal. The study highlights the importance of re-evaluating historical fossils with modern techniques, providing a more accurate understanding of human evolution in Europe.

INTRODUCTION

The Cannstatt fossil is thought to have been initially discovered near Uffkirche, Germany, in 1700 during an excavation ordered by Duke Eberhard Ludwig, undertaken due to the discovery of a mammoth tusk nearby (Adam 1973). This excavation yielded several remains, including mammoths, woolly rhinos, wild horses, and reindeer. The fossil and other materials discovered were all subsequently housed in Duke Kunst Kammer's collection (Adam 1989) but remained unstudied until 1835, when George Friedrich von Jäger rediscovered and described them. Among the finds was the Cannstatt fragmentary cranium, which von Jäger recognised as human (Jäger 1835). Despite this, the specimen did not receive significant attention in the scientific community at the time (Adam 1989). Darwin's theory of natural selection through his release of *On the Origin of Species* (Darwin 1864) had not yet been published, and evolution in general, as well as human evolution in particular, was not yet a mainstream scientific view.

Furthermore, there are some questions around its dis-

covery, as it has been stated to have been found in 1700, but it was not until 100 years later that Georg Friedrich von Jäger first described it and there is no documentation linking the skull to the 1700 excavation (Zängl-Kampf 1997), suggesting that its discovery may have occurred later, possibly between the mid-18th and early 19th centuries. As a result, the precise provenance and context of the fossil remain uncertain.

The status of the Cannstatt cranium changed when it was included in the influential publication "Crania Ethnica: les Crânes des races Humaines" by de Quatrefages and Hamy (1882). In this work, it was declared to be the prototype of a new hominin group, referred to as the 'race de Cannstatt'. This classification positioned the Cannstatt specimen alongside fossils such as Neanderthal 1 and La Naulette. While these specimens are today classified as Neanderthals (Schmitz et al. 2022; Toussaint and Leguebe 1984), others included in that grouping are now considered to represent *Homo sapiens*, possibly from the Upper Palaeolithic (e.g., Riquet 1972).

The classification of the Cannstatt fossil soon came under scrutiny. Notably, the German anatomist and anthropologist Gustav Schwalbe (1906) questioned its appointment as a distinct group. In his comparative study, some of the cranial differences between *H. sapiens* and Neanderthals were examined, which led him to conclude that the Cannstatt specimen was a modern human. His conclusion was based on several morphological features including the presence of a superciliary arch and planum supraorbitale (Schwalbe 1906). Schwalbe's study employed classical cranial measurements, including the cerebral index and the angle of the frontal bone, to support his argument. These methods provided a cranial analysis using the relative size and angles of different features to compare each specimen against each other to categorize the differences between *H. sapiens* and Neanderthals. These findings significantly impacted the perceived importance of the Cannstatt cranium. As it became increasingly regarded as a modern human, its perceived importance for our understanding of human evolution was reduced (Adam 1989).

Closely tied to the taxonomic interpretation of the Cannstatt cranium was the understanding of its geological age. Initially thought to be geologically relatively old, being described as a prehistoric human form, the fossil's chronology became a subject of debate (Adam 1989; Quatrefages and Hamy 1882). Berckhemer (1934) questioned the fossil's geological dating due to its fossilization patterns and the presence of Upper Paleolithic activity at the archaeological site where it was discovered. Again, this raised questions about the accuracy of its initial classification and its significance within the broader context of paleoanthropological research.

Unfortunately, little context remains for Cannstatt. It was found around faunal remains that suggested colder, ice age conditions (Jäger 1835). The mammoth fossil that was found in 1700 was initially interpreted as a unicorn fossil, prized for supposed healing powers (Adam 1973). Cannstatt was not even realized to be human until the collection was rediscovered in 1835 (Jäger 1835). While there was no direct evidence of butchery or hunting, the presence of large mammals and humans at the site has caused some suggestions that it was a Paleolithic hunting site (Adam 1973, 1989).

Today, two lineages are commonly recognized in the European Middle and Late Pleistocene human fossil record and are linked to Paleolithic assemblages. These include the Neanderthal lineage, which is considered to have evolved gradually in Eurasia from Middle Pleistocene forms referred to as *H. heidelbergensis* (e.g., Harvati and Reyes-Centeno 2022; Hublin 2009; see also Harvati et al. 2010). According to the 'Accretion Hypothesis' (Dean et al. 1998; Hublin 1998), Neanderthal traits evolved in a mosaic fashion through time, with the full suite of Neanderthal features, including the typical double arched continuous supraorbital torus and a low frontal bone squama (e.g., Harvati 2015) becoming established around Marine Isotope Stage (MIS) 7, or around 250 ka (Harvati et al. 2019; Hublin 2009). The *H. sapiens* lineage appeared later, with early Upper Paleolithic populations arriving in Europe by 45 ka (Hajdinjak et al. 2021; Prüfer et al. 2021)—although recent evidence suggests additional potential earlier incursions into Europe (e.g., at Mandrin, France, at ca. 54 ka, see Slimak et al. 2022; at Banyoles, Spain, at ca. 45–65 ka, see Keeling et al. 2023; Harvati et al. 2024; and at Apidima at ca. >210 ka, see Harvati et al. 2019). While recent *H. sapiens* is characterized by the gracile and discontinuous supraorbital region and a high, domed frontal bone squama, earlier representatives of the taxon, including Upper Paleolithic Europeans as well as basal *H. sapiens*, often show heavier and sometimes continuous supraorbital tori and less expanded frontal squama (e.g., Stringer 2016). This can be interpreted possibly as retention of ancestral features or as related to recent interbreeding with other hominin lineages, including Neanderthals in Europe (e.g., Harvati and Ackermann 2022). The temporal and geographic overlap, as well as extent of biological and cultural interaction between the two lineages remain hotly debated (e.g., Harvati and Ackermann 2022; Tsanova et al. 2024; Vallini et al. 2022), as does the general taxonomic status and phylogenetic affinities of the Middle Pleistocene *H. heidelbergensis sensu lato* (*s.l.*) (see e.g., Harvati and Reyes-Centenno 2022; Roksandic and Bae 2025). One severe limitation is the general scarcity of fossil remains (e.g., Harvati and Reyes-Centenno 2022; Vallini et al. 2022). In addition to new fieldwork and the discovery of new fossil remains, recent work has focused on the re-evaluation of existing specimens using modern approaches, either genetic or morphological, with the aim of clarifying their classification and relationships (e.g., Harvati et al. 2019, 2024; Keeling et al. 2023; Prüfer et al. 2021; Rmoutilová et al. 2018; Röding et al. 2021). This is also the goal of the present study.

The Cannstatt cranium was destroyed during bombing in the Second World War when on loan to anthropologist Theodore Mollison in Munich, drastically limiting the possibility of further study and verification of the fossil's characteristics and classification (Ziegler 1986). Its destruc-

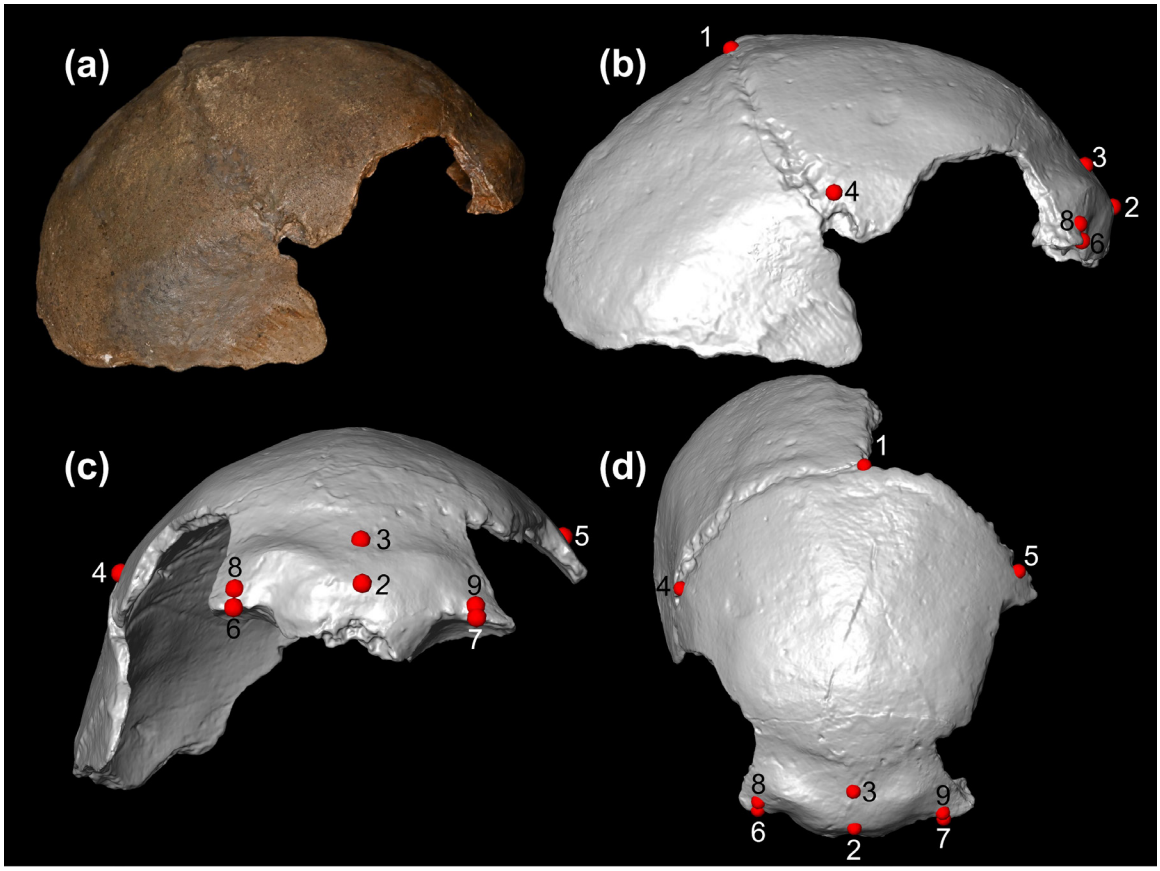


Figure 1. a) Photograph of the Cannstatt fossil (Adam 1989) with b) three images of its surface scan in lateral view, c) anterior view, and d) frontal-anterior oblique view. The surface scans also show the position of each of the landmarks placed (red).

tion has therefore left a gap in the historical and scientific record preventing aDNA analysis among other modern techniques, contributing to its status as an understudied and relatively obscure specimen in the field of paleoanthropology (Adam 1973, 1986, 1989). This study aims to reassess its affinities through a comparative shape analysis of its cast, using the toolkit of landmark-based geometric morphometrics (GMM) and focusing on its frontal bone (cf. Athreya 2006; White et al. 2022). Ultimately, this study aims to shed light on its potential significance in the broader context of Upper Paleolithic modern humans in Europe.

MATERIALS AND METHODS

SAMPLE

The forgotten, plaster cast of the original Cannstatt fossil was recently located in collections of the Stuttgart State Museum of Natural History by Achim Lehmkuhl (personal communication), another cast was also recently rediscovered in the Osteological collection of the University of Tübingen. The cast from the Stuttgart State Museum of Natural History was digitized using SHINING EinScan Pro HD and its accompanying software EXScan Pro 3.7.0.3, at a resolution of 0.25mm (Figure 1). The specimen preserves most of the frontal bone, with the exception of the lateral supraorbital regions, and part of the right parietal. Here we focus on the frontal bone, which is more complete and preserves several landmarks (homologous biological or structurally significant points on an object—Bookstein 1991; Slice 2007, Zelditch 2012) for analysis. The frontal bone has also been shown to be diagnostic for the classification of Pleistocene hominins (e.g., Athreya 2011; Mori et al. 2020).

A total of forty-six comparative specimens in the form of digital surface models were used in this study. They represented samples of recent *H. sapiens* (n=30), European Upper Paleolithic *H. sapiens* (n=7: Brno 2, Brünn 3, Grotte-Enfants 6, Mladeč 1, Mladeč 5, Předmostí 3, Předmostí 4), early *H. sapiens* (n=3: Skhul 5, Omo 1, Jebel Irhoud 1), *Homo neanderthalensis* (n=5: La Ferrassie 1, Neandertal 1, Guattari 1, Shanidar 1, Spy 1), *Homo heidelbergensis s.l.* (n=3: Arago 21, Sima de los Huesos 5, Petralona) (Table 1). Here, we follow Harvati and Reyes-Centeno (2022) and Meneganzin and Bernardi (2023) in recognizing Neanderthals as a distinct lineage, to which the taxonomic distinction of species can be applied, despite evidence for interbreeding with early *H. sapiens*.

GEOMETRIC MORPHOMETRICS

Nine homologous landmarks were identified on each frontal bone using the software AVIZO (Version 9.2 Lite,

TABLE 1. COMPARATIVE SPECIMENS USED IN THIS STUDY[1].

Specimen	Type of data	Classification
Arago 21*	Surface Scan	*Homo heidelbergensis*
Petralona	Medical Computed Tomography (CT) Scan, Museum of Geology, Paleontology and Paleoanthropology of the Aristotle University of Thessaloniki	*Homo heidelbergensis*
Sima de los Huesos 5*	Surface Scan	*Homo heidelbergensis*
Guattari 1*	Surface Scan	*Homo neanderthalensis*
La Ferrassie*	Surface Scan	*Homo neanderthalensis*
Neandertal 1*	Surface Scan	*Homo neanderthalensis*
Shanidar 1*	Surface Scan	*Homo neanderthalensis*
Spy 1	Surface Scan, Institut royal des Sciences naturelles de Belgique, Bruxelles NM Digital Archive	*Homo neanderthalensis*
Jebel Irhoud 1*	Surface Scan	Early *Homo sapiens*
Omo 1*	Surface Scan	Early *Homo sapiens*
Skhul 5	µCT Scan, Peabody Museum of Archaeology and Ethnology	Early *Homo sapiens*
Brno 2*	Surface Scan	European Upper Paleolithic *Homo sapiens*
Brünn 3*	Surface Scan	European Upper Paleolithic *Homo sapiens*
Grotte-Enfants 6*	Surface Scan	European Upper Paleolithic *Homo sapiens*
Mladeč 1	Medical CT Scan Natural History Museum Vienna, Anthropology Department	European Upper Paleolithic *Homo sapiens*
Mladeč 5*	Surface Scan	European Upper Paleolithic *Homo sapiens*
Předmostí 3*	Surface Scan	European Upper Paleolithic *Homo sapiens*
Předmostí*	Surface Scan	European Upper Paleolithic *Homo sapiens*
HD-Ber 2010/12 (Germany)	Surface Scan Kurpfälzisches Museum, Heidelberg	Recent *Homo sapiens* (sexes unknown)
Nusplingen (Germany) (n=7)	Surface Scan Paleoanthropology Osteological Collection of the University of Tübingen	Recent *Homo sapiens* (sexes unknown)
Vaihingen & Würtemberg (Germany) (n=22)	Surface Scan Paleoanthropology Osteological Collection of the University of Tübingen	Recent *Homo sapiens* (sexes unknown)

[1]Asterisks indicate specimens for which high quality casts were used from the collections of the American Museum of Natural History (New York), Department of Anthropology (New York), and Tübingen Osteological Collection.

TABLE 2. THE HOMOLOGOUS ECTOCRANIAL LANDMARKS THAT WERE IDENTIFIED FOR EACH OF THE COMPARATIVE SPECIMENS USED IN THIS STUDY.

Landmark	Location	Definition
Bregma - 1	midsagittal	The intersection between the sagittal and coronal sutures[1]
Glabella - 2	midsagittal	The point on the lower edge of the frontal bone, which is located above the frontonasal suture and between the superciliary arches. Measured at the most forward projecting point in the median sagittal plane (when the skull is oriented in the ear-eye plane)[1]
Post-toral sulcus - 3	midsagittal	Minima of concavity on midline post-toral frontal squama[2]
Stephanion – 4 & 5	bilateral	The intersection between the coronal suture and the temporal line[1]
Mid-orbit torus inferior –6 & 7	bilateral	The point on the inferior margin of the supraorbital torus in the middle of the orbit[2]
Mid-orbit torus superior –8 & 9	bilateral	The point on the superior aspect of the supraorbital torus in the middle of the orbit[2]

[1]Knußmann (1988)
[2]Harvati et al. (2010)

Thermo Fischer Scientific). Table 2 shows the landmarks used and their definitions (for illustration, see Figure 1b-d), which were chosen for their anatomical relevance for the cranial differences across all specimens.

The first step of the GMM analysis is a Generalized Procrustes Analysis (GPA). In this study, it was performed using the Morpho package (version 2.12, Schlager et al. 2023) in R (version 4.3.2). This standardized the specimens, aligning them by minimizing distances between corresponding landmarks so that there can be a statistical analysis of the resulting Procrustes shape coordinates (see e.g., Gunz et al. 2005; Harvati et al. 2019; Zelditch et al. 2012). In this process information about a specimen's orientation and location is removed, and landmark configurations are scaled to centroid size, the square root of the sum of squared distances from each landmark to the centroid (e.g., Zelditch et al. 2012).

ERROR CALCUALTIONS

An intra-observer error test was carried out by one of us (BC). Therefore, five individuals from the comparative sample were selected based on extremes of variation from a visual inspection, and the landmark set was digitized five times each over a week. The collected data were processed via GPA as described above and visualized in the form of a Principal Component Analyses (PCA) of all repeated measurements (Supplementary Information Figure S1). This PCA shows a successful error test, where the clusters for each individual have only a little variation between them, and considerable variation between clusters with none of them overlapping.

ANALYSIS

A PCA was then performed on the Procrustes-aligned coordinates using the geomorph package (version 4.0.7, Adams et al. 2024) in R. The Cannstatt fossil was projected into the PCA, which was based on the comparative sample, to determine its classification relative to the known species (e.g., Bosman et al. 2020; Röding et al. 2021; 2023). Three principal component plots (PC1 vs. PC2, PC1 vs. PC3, and PC2 vs. PC3) were generated to visualize the shape differences among the specimens. Convex hulls were used to show the ranges of each sample and were drawn around the extremes of each group. Deformed surfaces at ±2 sd of the PCs were produced to show shape changes along each PC axis.

In addition to the PCA, allometry was evaluated by visualizing the relationship between PC1 and centroid size as a measure of overall size and calculating a Pearson correlation test in PAST (version 4.03). The pairwise Procrustes distances of the landmark configurations of each individual measured compared to Cannstatt were also calculated for the recent *H. sapiens*, early *H. sapiens*, and Neanderthal groups (Harvati 2009).

For a statistical test to classify the Cannstatt crania, a discriminant function and classification analysis was performed in PAST to create a model where Cannstatt is assigned as unknown to predict how it would be classified.

In order to have more individuals in each group than variables, the *H. heidelbergensis* were removed from the analysis, and the early *H. sapiens*, and Upper Paleolithic *H. sapiens* were pooled into one group—Pre-modern *H. sapiens*. Although this group encompasses temporal and morphological diversity, its members broadly represent early examples of *H. sapiens* and share a diversity of ancestral and derived features. This grouping was not intended as a strict taxonomic category, but rather as a heuristic device to explore how the Cannstatt specimen relates morphologically to populations transitional between archaic forms and fully derived modern humans. For the statistical tests, PC 1-4 scores (accounting for 83.75% of the variation) were used. However, it is important to note that assumptions underlying the analysis, such as normality of the data, homogeneity of variance, and lack of multivariate collinearity, were not tested. A jack-knifed model was used, which resamples the data removing one individual from the dataset and evaluates whether the results change. This assesses the robustness of the classification analysis (Humphrey et al. 1999; Nicholson and Harvati 2006).

RESULTS

PRINCIPAL COMPONENTS ANALYSIS

The first principal component explained 54.07% of the variance. Individuals with a lower PC1 score have a slightly wider cranial shape along the transverse axis and rounder frontal squama with the temporal regions of the frontal bone extending less far posteriorly. In contrast, individuals with a higher PC1 score show a relatively more prominent supraorbital region with a deeper depression at the post-toral sulcus.

The second principal component explained 15.55% of the variance. Individuals with a lower PC2 score are relatively wider transversally and have a flatter frontal squama, also with a temporal region extending less posteriorly. In contrast, individuals with a higher PC2 score show a more prominent glabella as well as a more depressed post-toral sulcus.

The third principal component explained 8.36% of the variance. Individuals with a lower PC3 score seem to have a flatter, wider and more square-shaped frontal squama, whereas in the individuals with a higher PC3 score, it appears more rounded.

The first two PCs (together accounting for ca. 70% of the total variance) separate the groups relatively well, although extensive overlap exists between recent and Upper Paleolithic *H. sapiens*, as well as between *H. neanderthalensis* and early *H. sapiens*. Cannstatt is an outlier in this plot but plots closest to the convex hulls of our *H. sapiens* samples, which span a wide area of PC1. It is especially close the specimens Mladeč 5 and Omo 1, falling slightly above them on the plot (Figure 2). This high PC2 score could reflects Cannstatt's prominent glabella region.

When plotting PC1 against PC3 (Figure 3), our Neanderthal sample is largely distinct from all *H. sapiens* and *H. heidelbergensis s.l.* samples, with the exception of Sima de Los Huesos Cranium 5 falling into the *H. sapiens* variation. Similarly, the *H. heidelbergensis s.l.* sample overlaps in one case, Guattari, with the Upper Paleolithic *H. sapiens* convex hull. Where the main driver of this appears to be individuals with lower PC3 scores having a flatter, wider squamous region here, Cannstatt plots within the convex hulls of the European Upper Paleolithic *H. sapiens* but close to the region of overlap with Neanderthals and early *H. sapiens*.

Cannstatt plots well within the European Upper Paleolithic *H. sapiens* group when PC1 scores are plotted against centroid size (Figure 4). The centroid sizes of the groups tend to increase from modern to European Upper Paleolithic, to early *H. sapiens* and Neanderthals. The *H. heidelbergensis* individuals fall below that trend line, between the European Upper Paleolithic and early *H. sapiens* to Neanderthal range. An allometric component to PC1 was confirmed with a positive correlation between PC1 and centroid size (Pearson correlation test: $t=3.62$, DoF=47, $r=0.467$, $p<0.001$).

PAIRWISE PROCRUSTES DISTANCE

Figure 5 shows a plot with the spread of the pairwise Procrustes distances to Cannstatt within each group of the dataset. Cannstatt is closest to recent *H. sapiens* based on the median Procrustes distances, although the intra-group variation of recent *H. sapiens* is substantial. This is at least partially due to the larger sample size of this group relative to the others. The European Upper Paleolithic and early *H. sapiens* groups are also close to Cannstatt, and their spread of data is much narrower. Indeed, the early *H. sapiens* specimen Omo 1 is closest in overall shape to Cannstatt based on their pairwise Procrustes distance. The Neanderthal group shows higher Procrustes distances, although not statistically different from the *H. sapiens* samples. In contrast, all pairwise Procrustes distances to *H. heidelbergensis* fall above the observed variation for the early *H. sapiens* and Neanderthal samples and in the upper 25% of variation for the recent and Upper Paleolithic *H. sapiens*.

DISCRIMINANT FUNCTION ANALYSIS

The results of the discriminant function analysis using the scores from PC 1-4 are plotted in Figure 6. Cannstatt is an outlier in this plot but is closest to the convex hull of pre-modern *H. sapiens*. This model predicted the Cannstatt individual to be within the pre-modern *H. sapiens* group. The jack-knifed classification correctly classified 80% of the individuals, with the group that had the highest classification percentage being the recent *H. sapiens* with 93.33% correct (Table 3). The pre-modern *H. sapiens* group that Cannstatt was assigned to had a classification percentage of 40% (6 of the 10 were misclassified) suggesting its classification here may not be so reliable.

DISCUSSION

This study used geometric morphometrics to analyse the Cannstatt calvarium, a specimen whose classification has been debated. By comparing it to several Middle and Late Pleistocene hominins as well as recent *H. sapiens*, we

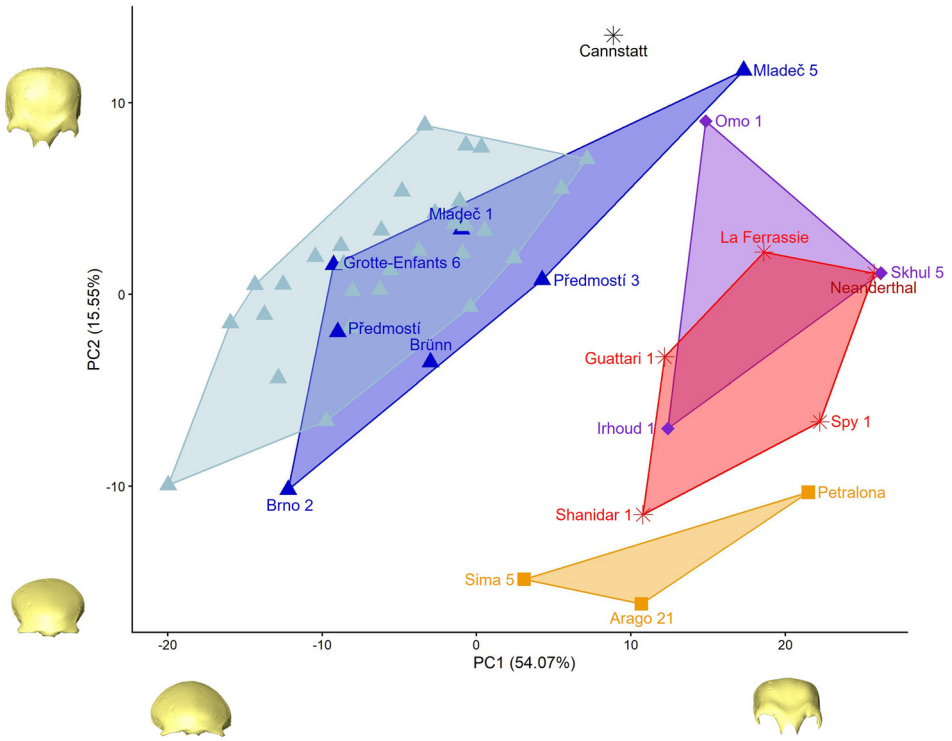


Figure 2. Principal components analysis for frontal bone shape—PC1 plotted against PC2 with Cannstatt (plotted in black) projected into the plot. Recent Homo sapiens *(n=30) are plotted in light blue, European Upper Paleolithic* H. sapiens *(n=7) are plotted in dark blue, early* H. sapiens *(n=3) are plotted in purple, Neanderthals (n=5) are plotted in red,* Homo heidelbergensis *(n=3) are plotted in orange. Shape changes along the axis for each PC are illustrations of surfaces ±2sd (frontal bone of individual 1106b from the Nusplingen collection).*

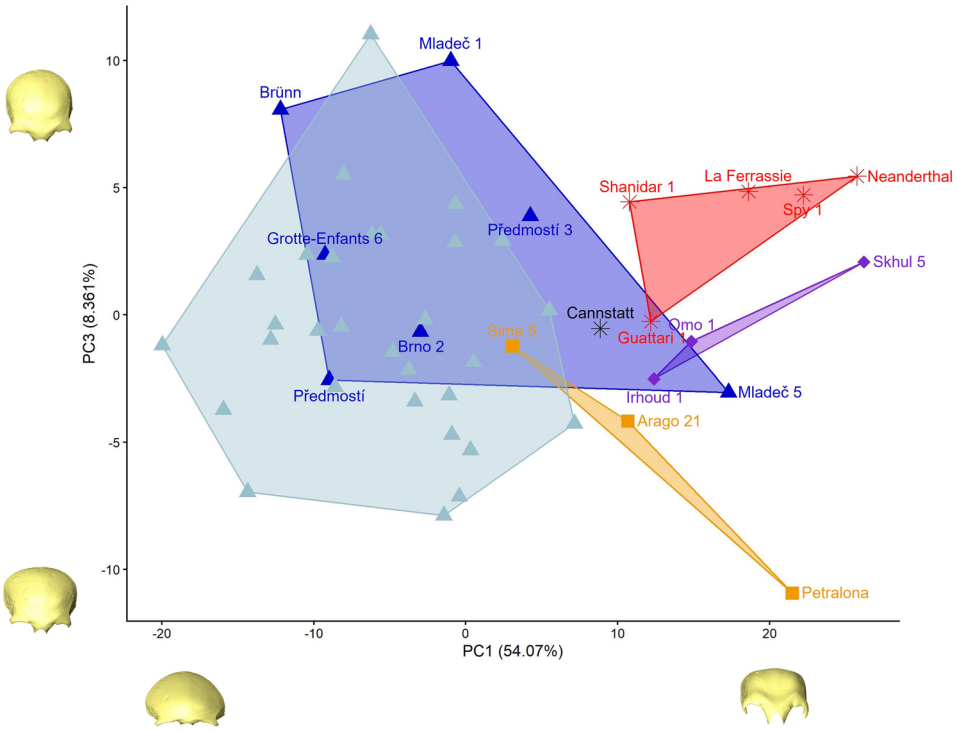


Figure 3. Principal components analysis for frontal bone shape—PC1 plotted against PC3 with Cannstatt projected into the plot. Symbols and colors are as in Figure 2.

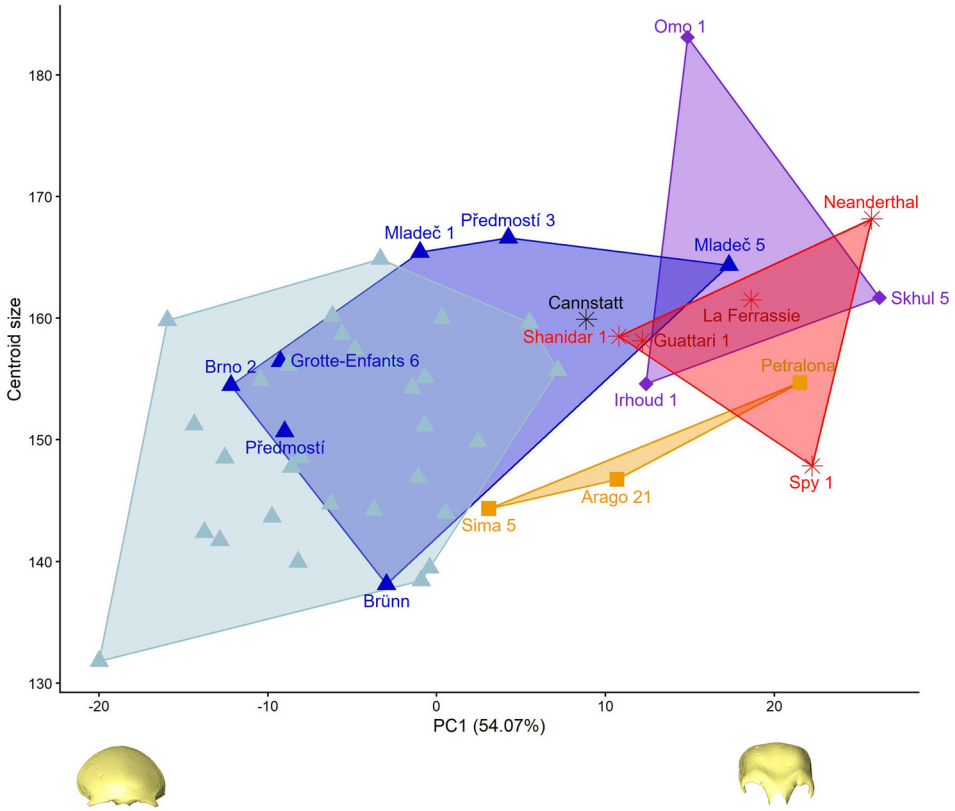


Figure 4. PC1 plotted against Centroid Size. Symbols and colors are as in Figure 2.

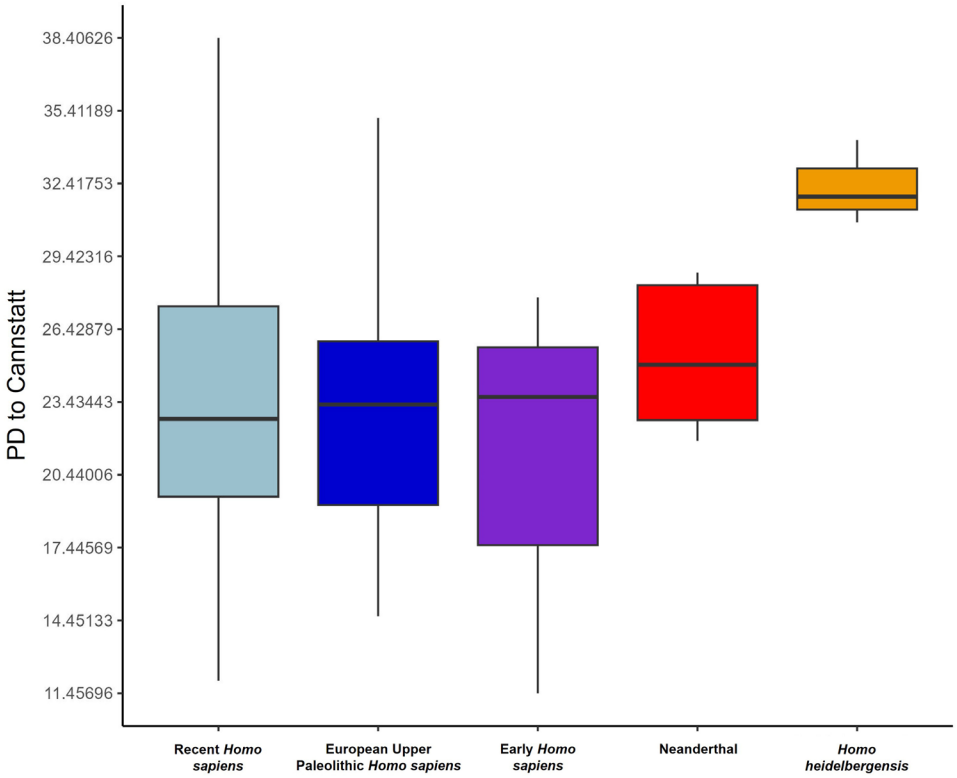


Figure 5. Box-whisker plot showing the Procrustes distance (PD) to Cannstatt of each of the recent Homo sapiens*, European Upper Paleolithic* H. sapiens*, early* H. sapiens*, Neanderthal, and* Homo heidelbergensis *samples. Colors for grouping used in this plot are as used in Figure 2.*

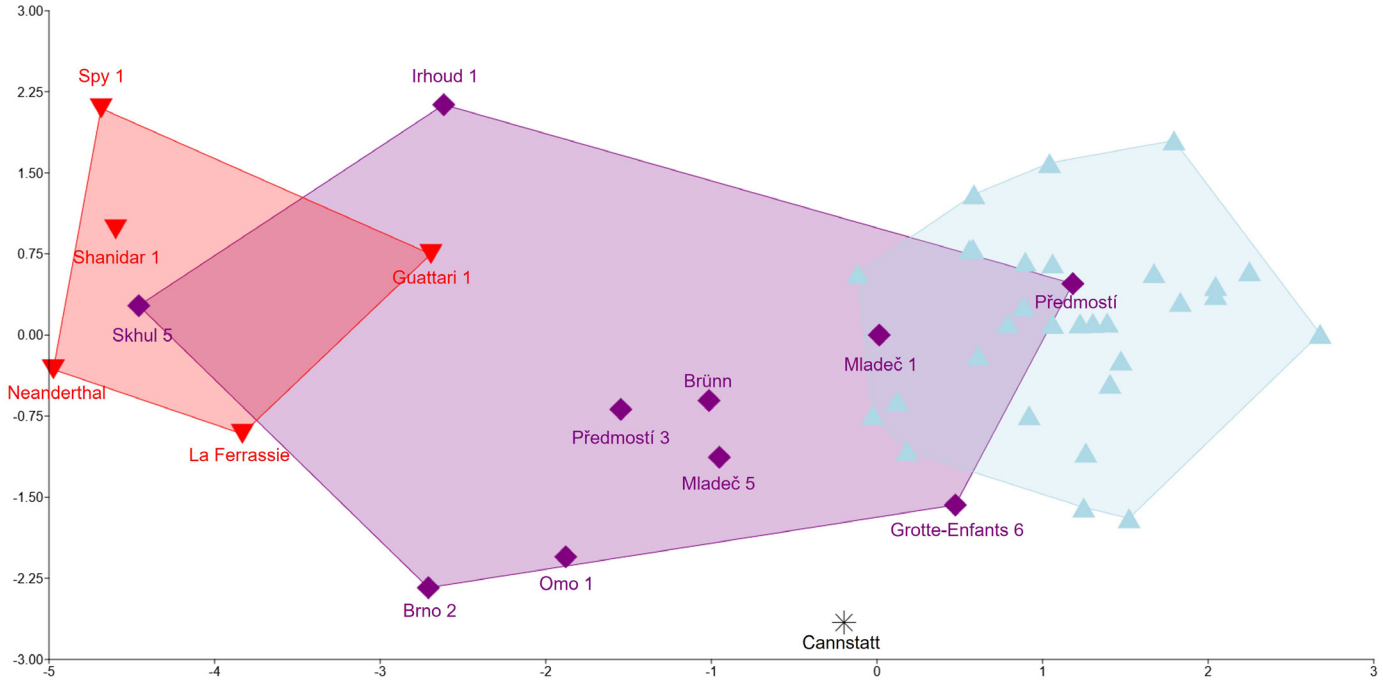


Figure 6. Plot of the results of the Discriminant Function analysis between the recent Homo sapiens *(light blue), pre-modern* H. sapiens *(dark purple), and Neanderthal (red) groups.*

aimed to help determine its affinities. The PCA revealed that Cannstatt plots consistently closest to *H. sapiens*, especially our Upper Paleolithic *H. sapiens* sample. Pairwise Procrustes distances further supported this finding, showing that recent *H. sapiens* had the closest median Procrustes distance to the Cannstatt specimen, followed by European Upper Paleolithic, and early *H. sapiens*. The discriminant function analysis provides additional support for these results, classifying Cannstatt as a pre-modern *H. sapiens*.

Our findings support Schwalbe's (1906) conclusion that the Cannstatt specimen is a representative of *H. sapiens* rather than a Neanderthal or other hominin species. Schwalbe's classification was based on traditional morphological features such as the superciliary arch and the frontal bone angle, which he found to be characteristic of recent *H. sapiens*. The results of our 3D geometric morphometrics analysis of Cannstatt's frontal bone shape, reinforce this assessment with modern methods. Our findings also suggest that some of the more basal features that align Cannstatt with Upper Paleolithic or early *H. sapiens* on PC1, such as the prominent glabella, may be related to size, as PC1 includes an allometric component. This allometric relationship may also partly explain the overlap on PC1 of early *H. sapiens* specimens such as Irhoud 1 and Skhul 5, which are both considered to have relatively robust supraorbital regions (Gunz et al. 2009) as well as of the early Upper Paleolithic specimen Mladeč 5, which is also considered to be relatively robust (Weber et al. 2006), with our Neander-

TABLE 3. CROSS VALIDATION RESULTS FROM THE DISCRIMINANT FUNCTION ANALYSIS SHOWING THE NUMBER OF ACTUAL AND PREDICTED RESULTS FOR THE INDIVIDUALS IN EACH GROUPING.

		Actual		
		Pre-modern *H. sapiens*	Neanderthal	Recent *H. sapiens*
Predicted	Pre-modern *H. sapiens*	4	1	2
	Neanderthal	3	4	0
	Recent *H. sapiens*	3	0	28

thal sample. To what extent such morphology may also be influenced by genetic factors through interbreeding with Neanderthals (see, e.g., Gunz et al. 2019; Harvati and Ackermann 2022) is unclear. Cannstatt does not plot close to *H. heidelbergensis*, as expected from previous work identifying the specimen as a modern human. Figure 5 shows this particularly well where its Procrustes distances are greatest from the *H. heidelbergensis* individuals.

This study, albeit limited, contributes to the known evidence on human evolution in Europe in the late Pleistocene, a period of coexistence and interaction between hominin populations. The classification of the Cannstatt fossil as *H. sapiens* is consistent with previous work on this specimen. If we assume an Upper Paleolithic age, its retention of some archaic features can be interpreted as retention of basal traits from earlier ancestral populations, or through potential recent admixture with Neanderthal populations (Green et al. 2010; Harris and Nielsen 2016; Harvati and Ackermann 2022; Meyer et al. 2012; Prüfer et al. 2014). However, a later chronology, and the possibility that these features are related to its large size alone, cannot be excluded.

This study is limited by several factors, the most important of which are the lack of contextual information for the specimen, which severely limits its interpretation, and the use of a cast, rather than the original, in our analysis. This was necessary, since the original was destroyed and is no longer available. Although we cannot exclude that some deformation might have taken place in the intervening years since the cast was produced, no obvious asymmetries or other anomalies were observed, leading us to believe that if such deformation occurred, it likely would not greatly influence our results. Additionally, an important limitation is the small dataset, particularly with regard to the fossil samples included. An expanded sample, especially of Upper Paleolithic individuals, may help further assess the hypothesis that Cannstatt is a representative of these early Europeans. Furthermore, the current study focused on the frontal bone, excluding the parietal morphology. The right parietal is partially preserved but does not preserve a sufficient number of landmarks for inclusion in this study. Future work including the parietal should be conducted to further evaluate our results, as the parietals contribute to the overall shape of the skull influencing cranial width, and height, therefore allowing for more comprehensive analysis of cranial variation. Another limitation of this study is the broad and heterogeneous nature of the "pre-modern *H. sapiens*" group, which includes individuals from varying regions and time periods, ranging from 300 ka to 30 ka. While these specimens share general similarities as *H. sapiens*, they also show considerable morphological variation, reflecting different evolutionary stages and local adaptations. This group should be interpreted as a useful tool for comparative purposes rather than a precise taxonomic group. Finally, several of the landmarks used in this study do not represent Type I landmarks (Bookstein 1990) and therefore are potentially prone to a higher degree of error, a problem which is compounded here by the fragmentary nature of the specimen, which, additionally, is only represented by a cast. This issue may complicate the interpretation of our findings. The future use of new methods, such as surface registration for shape analysis (e.g., Röding et al. 2023), which is largely independent of landmarks, would circumvent these issues and provide a more comprehensive view of the surface morphology of this specimen. Finally, any conclusive reinterpretation of this specimen must also take its geological and cultural context into account, something that can only be clarified with a combination of archival investigation and new fieldwork at the site.

CONCLUSION

In conclusion, we have used landmark-based 3D geometric morphometrics to re-evaluate the Cannstatt specimen. Our results confirm its previous classification as *H. sapiens* and provide tentative support for a potential attribution to Upper Paleolithic Europeans. The results highlight the importance of revisiting historical finds with modern techniques. Future work should expand to include surface analysis of both the frontal and the parietal bone, as well as consider the specimen's geological and cultural context, for a more secure interpretation.

ACKNOWLEDGMENTS

We thank the Kurpfälzische Museum Heidelberg, and Eric Delson and the NYCEP morphometrics group for providing access to surface scans. We would also like to thank Eli Amson for his help with this project. This work was supported by the Deutsche Forschungsgemeinschaft Gottfried Wilhelm Leibniz award (2021) and the European Research Council ERC AdG 101019659, both awarded to KH. KH is also supported by the Carl Friedrich von Siemens Foundation. AH was also supported by a scholarship from CNPq (Conselho Nacional de Desenvolvimento Científico e Tecnológico). We thank two anonymous reviewers for their helpful comments and suggestions, which greatly improved our manuscript.

DATA AVAILABILITY

The dataset used will be made available at the Zenodo depository upon publication (https://zenodo.org/records/19498446).

CONFLICT OF INTEREST STATEMENT

The authors declare no conflict of interest.

AUTHOR CONTRIBUTIONS

Conceptualization: CR, AH, KH; Data curation: BC, CR; Formal analysis: BC; Funding acquisition: KH; Investigation: BC; Methodology: CR, KH; Project administration: KH; Visualization: BC; Writing (original draft): BC, KH; Writing (review & editing): BC, CR, AH, KH

USE OF GENERATIVE AI STATEMENT

No generative AI was use when writing this article. AI tools for translating scientific papers (DeepL) in other languages were used to assist writing the article.

This work is distributed under the terms of a Creative Commons Attribution-NonCommercial 4.0 Unported License.

REFERENCES

Adam, K.D., 1973. Anfänge urgeschichtlichen Forschens in Südwestdeutschland. Quartär 23/24., 21–36.

Adam, K.D., 1986. Schrifttum zur Erforschung der Stuttgarter Travertine. Fundber. Baden-Württ. 11, 92–100.

Adam, K.D., 1989. Alte und neue Urmenschen-Funde in Südwestdeutschland-eine kritische Würdigung. Quartär 39/40, 177–190.

Adams, D.C., Collyer, M.L., Kaliontzopoulou, A., Baken, E.K., 2024. geomorph: Geometric Morphometric Analyses of 2D and 3D Landmark Data, version 4.0.7. Available at: https://cran.r-project.org/package=geomorph

Athreya, S., 2006. Patterning of geographic variation in Middle Pleistocene *Homo* frontal bone morphology. J. Hum. Evol. 50, 627–643

Athreya, S., 2011. South Asia as a geographic crossroad: patterns and predictions of hominin morphology in Pleistocene India. In: Norton, C., Braun, D. (Eds.), Asian Paleoanthropology: From Africa to China and Beyond. Springer, Dordrecht, pp. 129–141.

Berckhemer, F., 1934. Der Steinheimer Urmensch und die Tierwelt seines Lebensgebietes. Aus der Heimat 47, 101–115.

Bookstein, F.L., 1990. Introduction to methods for landmark data. In: Rohlf, F.J., Bookstein, F.L. (Eds.), Proceedings of the Michigan Morphometrics Workshop. The University of Michigan Museum of Zoology, Ann Arbor, MI, pp. 215–226.

Bookstein, F.L., Grayson, B., Cutting, C.B., Kim, H.-C., McCarthy, J.G., 1991. Landmarks in three dimensions: reconstruction from cephalograms versus direct observation. Am. J. Orthod. Dentofac. Orthop. 100, 133–140.

Bosman, A.M., Reyes-Centeno, H., Harvati, K., 2020. A virtual assessment of the suprainiac depressions on the Eyasi I (Tanzania) and Aduma ADU-VP-1/3 (Ethiopia) Pleistocene hominin crania. J. Hum. Evol. 145, 102815.

Darwin, C., 1859. XI: Geographical Distribution. In: Darwin, C., On the Origin of Species by Means of Natural Selection, or the Preservation of Favoured Races in the Struggle for Life. W. Clowes and Sons, London.

Dean, D., Hublin, J.-J., Holloway, E., 1998. On the phylogenetic position of the pre-Neandertal specimen from Reilingen, Germany. J. Hum. Evol. 34, 485–508

Green, R.E., Krause, J., Briggs, A.W., Maricic, T., Stenzel, U., Kircher, M., Patterson, N., Li, H., Zhai, W., Hsi-Yang Fritz, M., Hansen, N.F., Durand, E.Y., Malaspinas, A.-S., Jensen, J.D., Marques-Bonet, T., Alkan, C., Prüfer, K., Meyer, M., Burbano, H.A., Good, J.M., Schultz, R., Aximu-Petri, A., Butthof, A., Höber, B., Höffner, B., Siegemund, M., Weihmann, A., Nusbaum, C., Lander, E.S., Russ, C., Novod, N., Affourtit, J., Egholm, M., Verna, C., Rudan, P., Brajkovic, D., Kucan, Ž., Gušic, I., Doronichev, V.B., Golovanova, L.V., Lalueza-Fox, C., de la Rasilla, M., Fortea, J., Rosas, A., Schmitz, R.W., Johnson, P.L.F., Eichler, E.E., Falush, D., Birney, E., Mullikin, J.C., Slatkin, M., Nielsen, R., Kelso, J., Lachmann, M., Reich, D., Pääbo, S., 2010. A draft sequence of the Neandertal genome. Science 328, 710–722.

Gunz, P., Bookstein, F.L., Mitteroecker, P., Stadlmayr, A., Seidler, H., Weber, G.W., 2009. Early modern human diversity suggests subdivided population structure and a complex out-of-Africa scenario. Proc. Nat. Acad. Sci. U.S.A. 106, 6094–6098.

Gunz, P., Mitteroecker, P., Bookstein, F.L., 2005. Semilandmarks in three dimensions. In: Slice, D.E. (Ed.), Modern Morphometrics in Physical Anthropology. Springer, New York, pp. 73–98.

Harvati, K. Hublin, J.J. and Gunz, P., 2010. Evolution of middle-late Pleistocene human cranio-facial form: a 3-D approach. J. Hum. Evol. 59(5), 445–464.

Gunz, P., Tilot, A.K., Wittfeld, K., Teumer, A., Shapland, C.Y., Van Erp, T.G., Dannemann, M., Vernot, B., Neubauer, S., Guadalupe, T., 2019. Neandertal introgression sheds light on modern human endocranial globularity. Curr. Biol. 29, 120–127.

Hajdinjak, M., Mafessoni, F., Skov, L., Vernot, B., Hübner, A., Fu, Q., Essel, E., Nagel, S., Nickel, B., Richter, J., Moldovan, O. T., Constantin, S., Endarova, E., Zahariev, N., Spasov, R., Welker, F., Smith, G. M., Sinet-Mathiot, V., Paskulin. L., Fewlass, H., Talamo, S., Rezek, Z., Sirakova, S., Sirakov, N., McPherron, S. P., Tsanova, T., Hublin, J.-J., Peter, B. M., Meyer, M., Skoglund, P., Kelso, J., Pääbo, S., 2021. Initial Upper Palaeolithic humans in Europe had recent Neanderthal ancestry. Nature 592, 253–257. https://doi.org/10.1038/s41586-021-03335-3

Harris, K., Nielsen, R., 2016. The genetic cost of Neanderthal introgression. Genetics 203(2), 881–891.

Harvati, K., 2009. Into Eurasia: a geometric morphometric re-assessment of the Upper Cave (Zhoukoudian) specimens. J. Hum. Evol. 57, 751–762.

Harvati, K., 2015. Neanderthals and their contemporaries. In: Henke, W., Tattersall, I. (Eds.) Handbook of Paleoanthropology, 2nd Edition. Springer, Berlin, Heidelberg, pp. 2243–2279

Harvati, K., Ackermann, R.R., 2022. Merging morphological and genetic evidence to assess hybridization in Western Eurasian late Pleistocene hominins. Nat. Ecol. Evol. 6, 1573–1585.

Harvati, K., Hublin, J.J., Gunz, P., 2010. Evolution of middle-late Pleistocene human cranio-facial form: a 3-D approach. J. Hum. Evol. 59(5), 445–464.

Harvati, K., Reyes-Centeno, H., 2022. Evolution of *Homo* in the Middle and Late Pleistocene. J. Hum. Evol. 173, 103279.

Harvati, K., Röding, C., Bosman, A.M., Karakostis, F.A., Grün, R., Stringer, C., Karkanas, P., Thompson, N.C., Koutoulidis, V., Moulopoulos, L.A., Gorgoulis, V.G., Kouloukoussa, M., 2019. Apidima Cave fossils provide earliest evidence of *Homo sapiens* in Eurasia. Nature 571, 500–504.

Harvati, K., Stringer, C., Folorunso, C.A., 2024. Comparative 3D Shape analysis of the Iwo Eleru Mandible, Ni-

geria. PaleoAnthropology 2024:1, 99–111.

Hawks, J.D., Wolpoff, M.H., 2001 The Accretion Model of Neanderthal evolution. Evolution 55, 1474–1485

Hublin, J.-J. 1998. Climatic changes, paleogeography and the evolution of Neanderthals. In: Aoki, K., Bar-Yosef, O. (Eds.), Neanderthals and Modern Humans in Western Asia. Plenum Press, New York, pp. 295–310.

Hublin, J.J., 2009. The origin of Neandertals. Proc. Nat. Acad. Sci. U.S.A. 106, 16022–16027.

Humphrey, L.T., Dean, M.C., Stringer, C.B., 1999. Morphological variation in great ape and modern human mandibles. J. Anat. 195, 491–513.

Jäger, G.F. von, 1835. Über die fossilen Säugetiere, welche in Württemberg in verschiedenen Formationen aufgefunden worden sind, nebst geognostischen Bemerkungen über diese Formationen. Metzler, Stuttgart.

Keeling, B.A., Quam, R., Martínez, I., Arsuaga, J.L., Maroto, J., 2023. Reassessment of the human mandible from Banyoles (Girona, Spain). J. Hum. Evol. 174, 103291.

Knußmann, R., 1988. Handbuch der Vergleichenden Biologie des Menschen. Aufl., Bd. I: Wesen und Methoden der Anthropologie. Gustav Fischer Verlag, Stuttgart.

Meneganzin, A., Bernardi, M., 2023. Were Neanderthals and *Homo sapiens* 'good species'? Quatern. Sci. Rev. 303, 107975.

Mitteroecker, P., Gunz, P., 2009. Advances in geometric morphometrics. Evol. Biol. 36, 235–247.

Mori, T. Profico, A. Reyes-Centeno, H., Harvati, K., 2020. Frontal bone virtual reconstruction and geometric morphometric analysis of the mid-Pleistocene hominin KNM-OG 45500 (Olorgesailie, Kenya). J. Anthropol. Sci. 98, 49–72.

Nicholson, E., Harvati, K., 2006. Quantitative analysis of human mandibular shape using three-dimensional geometric morphometrics. Am. J. Phys. Anthropol. 131, 368–383.

Prüfer, K., Posth, C., Yu, H., Stoessel, A., Spyrou, M.A., Deviese, T., Mattonai, M., Ribechini, E., Higham, T., Velemínskỳ, P., 2021. A genome sequence from a modern human skull over 45,000 years old from Zlatỳ kůň in Czechia. Nat. Ecol. Evol. 5, 820–825.

Prüfer, K., Racimo, F., Patterson, N., Jay, F., Sankararaman S., 2014. The complete genome sequence of a Neanderthal from the Altai Mountains. Nature 505, 43–49

Quatrefages, A. de, Hamy, E., 1882. Première race humaine fossile ou race de Canstadt. In: Crania ethnica. Les crânes des races humaines décrits et figurés d'après les collections du Muséum d'histoire naturelle de Paris, de la société d'anthropologie de Paris et les principales collections de la France et de l'étranger. J. B. Baillière, Paris, pp. 1–43.

Riquet, R., 1972. Quelques documents réputés paléolithiques. Bull. Mém. Soc. Anthropol. Paris 9, 135–160.

Rmoutilová, R., Guyomarc'h, P., Velemínskỳ, P., Šefčáková, A., Samsel, M., Santos, F., Maureille, B., Brůžek, J., 2018. Virtual reconstruction of the Upper Palaeolithic skull from Zlatỳ kůň, Czech Republic: sex assessment and morphological affinity. PloS One 13, e0201431.

Röding, C., Stringer, C., Lacruz, R.S., Harvati, K., 2023. Mugharet el'Aliya: affinities of an enigmatic north African Aterian maxillary fragment. Am. J. Biol. Anthropol. 180, 352–369.

Röding, C., Zastrow, J., Scherf, H., Doukas, C., Harvati, K., 2021. Crown outline analysis of the hominin upper third molar from the Megalopolis Basin, Peloponnese, Greece. In: Reyes-Centeno, H., Harvati, K. (Eds.), Ancient Connections in Eurasia. Kerns Verlag, Tübingen, pp. 13–36.

Schlager, S., Jefferis, G., Dryden, I., 2023. Morpho: Calculations and Visualisations Related to Geometric Morphometrics, version 2.12. Available at: https://cran.r-project.org/package=Morpho

Schmitz, R.W., Serre, D., Bonani, G., Feine, S., Hillgruber, F., Krainitzki, H., Pääbo, S., Smith, F.H., 2002. The Neandertal type site revisited: interdisciplinary investigations of skeletal remains from the Neander Valley, Germany. Proc. Nat. Acad. Sci. 99, 13342–13347.

Schwalbe, G., 1906. Studien zur Vorgeschichte des Menschen. E. Nägele, Stuttgart, pp. 183–228.

Slice, D.E., 2007. Geometric morphometrics. Ann. Rev. Anthropol. 36, 261–281.

Stringer, C., 2016. The origin and evolution of *Homo sapiens*. Phil. Trans. R. Soc. B 371, 20150237.

Toussaint, M., Leguebe, A., 1984. Morphologie et morphométrie des restes humains de La Naulette (Belgique). C. R. Séances Acad. Sci. Sér. II 299, 1363–1368.

Tsanova, T., Delvigne, V., Sirakova, S., Anastasova, E., Horta, P., 2024. Curated character of the Initial Upper Palaeolithic lithic artefact assemblages in Bacho Kiro Cave (Bulgaria). PloS One 19(9), e0307435.

Vallini, L., Marciani, G., Aneli. S., Bortolini, E., Benazzi, S., Pievani, T., Pagani, L. 2022. Genetics and material culture support repeated expansions into Paleolithic Eurasia from a population hub out of Africa. Genome Biol. Evol. 14(4), evac045.

Weber, G.W., Gunz, P., Mitteröcker, P., Stadlmayr, A., Bookstein, F.L., Seidler, H., 2006. External geometry of Mladeč neurocrania compared with anatomically modern humans and Neandertals. In: Teschler-Nicola, M. (Ed.), Early Modern Humans at the Moravian Gate. Springer Vienna, Vienna, pp. 453–471.

White, S., Pope, M., Hillson, S., Soligo, C., 2022. Geometric morphometric variability in the supraorbital and orbital region of Middle Pleistocene hominins: implications for the taxonomy and evolution of later *Homo*. J. Hum. Evol. 162, 103095.

Zängl-Kampf, U., 1997. Cannstatt Skull. In: Spencer, F. (Ed.), History of Physical Anthropology: An Encyclopedia. Garland Publishing, New York, pp. 254–256.

Zelditch, M., Swiderski, D.L., Sheets, H.D., 2012. Geometric Morphometrics for Biologists: A Primer (2nd edition). Academic Press, Amsterdam, London.

Ziegler, B., 1986. Das menschliche Schädeldach von Cannstatt. Konrad Theiss, Stuttgart, pp. 32-34.

Supplement 1 to Re-Evaluating the Cannstatt Cranium (Germany): Using Geometric Morphometrics to Assess a Lost Presumed Human Fossil

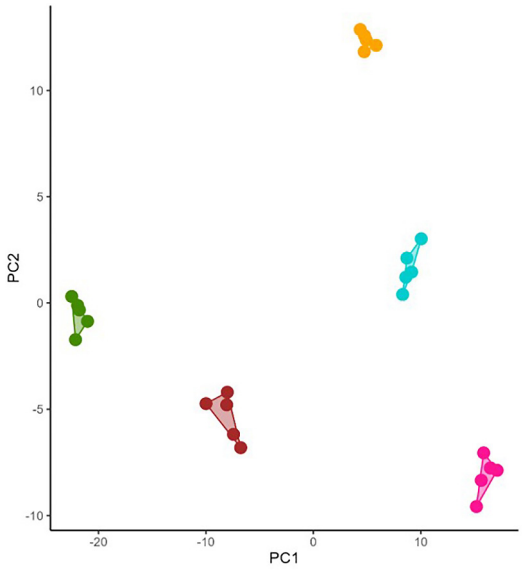
BENJAMIN CHAMBERLAIN
Palaeoanthropology, Institute for Archaeological Sciences, Eberhard Karls Universität Tübingen; and, Senckenberg Centre for Human Evolution and Palaeoenvironment, Eberhard Karls Universität Tübingen, Tübingen, GERMANY; ben.j.chamberlain@gmail.com

CAROLIN RÖDING
Palaeoanthropology, Institute for Archaeological Sciences, Eberhard Karls Universität Tübingen; and, Senckenberg Centre for Human Evolution and Palaeoenvironment, Eberhard Karls Universität Tübingen, Tübingen, GERMANY; carolin.roeding@uni-tuebingen.de

ALEX HUBBE
Staatliches Museum für Naturkunde Stuttgart, Rosenstein 1, 70191 Stuttgart, GERMANY; Departamento de Oceanografia, Instituto de Geociências, Universidade Federal da Bahia, R. Barão de Jeremoabo, S/N, 40170-020 Salvador, BA; and Instituto do Carste, Rua Barcelona 240/302, 30360-260 Belo Horizonte, MG, BRAZIL; alexhubbe@yahoo.com

KATERINA HARVATI
Paleoanthropology, Institute for Archaeological Sciences, Eberhard Karls Universität Tübingen; and, Senckenberg Center for Human Evolution and Paleoenvironments, Eberhard Karls Universität Tübingen; DFG Center for Advanced Studies 'Words, Bones, Genes, Tools', Eberhard Karls Universität Tübingen; HUMAN ORIGINS – Cluster of Excellence for Integrative Human Origins Studies (EXC 3101), Eberhard Karls University of Tübingen, Tübingen, GERMANY; Centre for Early Sapiens Behaviour (SapienCE), University of Bergen, NORWAY; and, Museum of Anthropology, Medical School, National and Kapodistrian University of Athens, Athens, GREECE; katerina.harvati@ifu.uni-tuebingen.de

SUPPLEMENT 1
This supplement contains: Supplementary Information Figure S1.



Supplementary Figure 1. Principal components analysis for frontal bone shape for landmark error test—PC1 plotted against PC2. Each individual was measured five times over a week for the landmarks shown in Figure 1. Cannstatt is plotted in brown. Mladeč 1 is plotted in pink, Neanderthal 1 is plotted in green, individual 803 from the Vaihingen & Würtemberg collection is plotted in cyan, and individual 1124 from the Nusplingen collection is plotted in orange.